Electrostatic interactions between middle domain motif-1 and the AAA1 module of the bacterial ClpB chaperone are essential for protein disaggregation

Received for publication, August 22, 2018, and in revised form, October 11, 2018 Published, Papers in Press, October 16, 2018, DOI 10.1074/jbc.RA118.005496

Saori Sugita[‡1], Kumiko Watanabe[‡1], Kana Hashimoto[‡], Tatsuya Niwa[§], Eri Uemura[§], Hideki Taguchi[§], and Yo-hei Watanabe[‡¶2]

From the [‡]Department of Biology, Faculty of Science and Engineering and [¶]Institute for Integrative Neurobiology, Konan University, Okamoto 8-9-1, Kobe 658-8501 and the [§]Cell Biology Center, Institute of Innovative Research, Tokyo Institute of Technology, 4259 Nagatsuta-cho, Midori-ku, Yokohama 226-8503, Japan

Edited by Ursula Jakob

ClpB, a bacterial homologue of heat shock protein 104 (Hsp104), can disentangle aggregated proteins with the help of the DnaK, a bacterial Hsp70, and its co-factors. As a member of the expanded superfamily of ATPases associated with diverse cellular activities (AAA^+), ClpB forms a hexameric ring structure, with each protomer containing two AAA^+ modules, AAA1 and AAA2. A long coiled-coil middle domain (MD) is present in the C-terminal region of the AAA1 and surrounds the main body of the ring. The MD is subdivided into two oppositely directed short coiled-coils, called motif-1 and motif-2. The MD represses the ATPase activity of ClpB, and this repression is reversed by the binding of DnaK to motif-2. To better understand how the MD regulates ClpB activity, here we investigated the roles of motif-1 in ClpB from *Thermus thermophilus* (*T*ClpB). Using systematic alanine substitution of the conserved charged residues, we identified functionally important residues in motif-1, and using a photoreactive cross-linker and LC-MS/MS analysis, we further explored potential interacting residues. Moreover, we constructed *T*ClpB mutants in which functionally important residues in motif-1 and in other candidate regions were substituted by oppositely charged residues. These analyses revealed that the intra-subunit pair Glu-401–Arg-532 and the inter-subunit pair Asp-404–Arg-180 are functionally important, electrostatically interacting pairs. Considering these structural findings, we conclude that the Glu-401–Arg-532 interaction shifts the equilibrium of the MD conformation to stabilize the activated form and that the Arg-180–Asp-404 interaction contributes to intersubunit signal transduction, essential for ClpB chaperone activities.

ClpB/Hsp104 is a protein disaggregase required for thermotolerance of cells (1–3). To disentangle aggregated proteins, ClpB/Hsp104 cooperates with DnaK/Hsp70 chaperone and its co-factors, DnaJ/Hsp40, and the nucleotide exchange factor, GrpE (4–7).

As a member of an expanded superfamily of ATPases associated with diverse cellular activities (AAA^+), ClpB/Hsp104 contains two AAA^+ modules, AAA1 and AAA2, in a polypeptide and forms a hexameric ring-like structure, in which each AAA^+ module constitutes each layer of a two layered ring (8). At the top of the ring, highly mobile globular N-terminal domains (ND)[3] contribute to bind protein aggregates (9, 10), and long coiled-coil middle domains (MD) protruding from the C-terminal small subdomain of the AAA1 modules surround the main body of the ring (Fig. 1*a*) (8). The MD is subdivided into two oppositely-directed short coiled-coils, motif-1 and motif-2.

Both the AAA1 and AAA2 modules bind and hydrolyze ATP in a complex cooperative manner that contains intra- and inter-ring cooperation (11–13). The structural changes of the ring, induced by the cooperative ATPase cycle, promote disentangling of aggregated substrates by threading them into the central pore of the ring. Recent cryo-electron microscopy (cryo-EM) and high-speed atomic force microscopy analyses demonstrated that the structural inter-conversion between the hexameric ring, spiral, and twisted half-spiral structures occurred during the ATPase cycle and contributed to the disaggregation reaction (14–17).

Ordinarily, the MD represses the ATPase activity of ClpB/Hsp104 by an unknown mechanism (18, 19). In addition, the binding affinity of ClpB/Hsp104 for aggregation is not high enough to start threading (20). To perform disaggregation, the recruitment of ClpB/Hsp104 to the aggregates and the cancellation of repression are required (21). DnaK/Hsp70 consists of an N-terminal nucleotide-binding domain (NBD) and a substrate-binding domain (SBD) (22, 23). The NBD controls the conformation of the SBD and its binding affinity for substrate proteins in an ATPase cycle-dependent manner (24, 25). In the high-affinity conformation, the NBD can bind to the edge of MD motif-2 of ClpB/Hsp104 (21, 26). This interaction causes

This work was supported by JSPS KAKENHI Grants 24241048 and 26440085. The authors declare that they have no conflicts of interest with the contents of this article.

[1] Both authors contributed equally to this work.

[2] To whom correspondence should be addressed: Dept. of Biology, Faculty of Science and Engineering, Konan University, Okamoto 8-9-1, Kobe 6588501, Japan. Tel./Fax: 81-78-435-2514; E-mail: ywatanab@center.konan-u.ac.jp.

[3] The abbreviations used are: ND, N-terminal domain; MD, middle domain; BPM, benzophenone-4-maleimide; NBD, nucleotide-binding domain; SBD, substrate-binding domain; PDB, Protein Data Bank; TCEP, tris(2-carboxyethyl)phosphine.

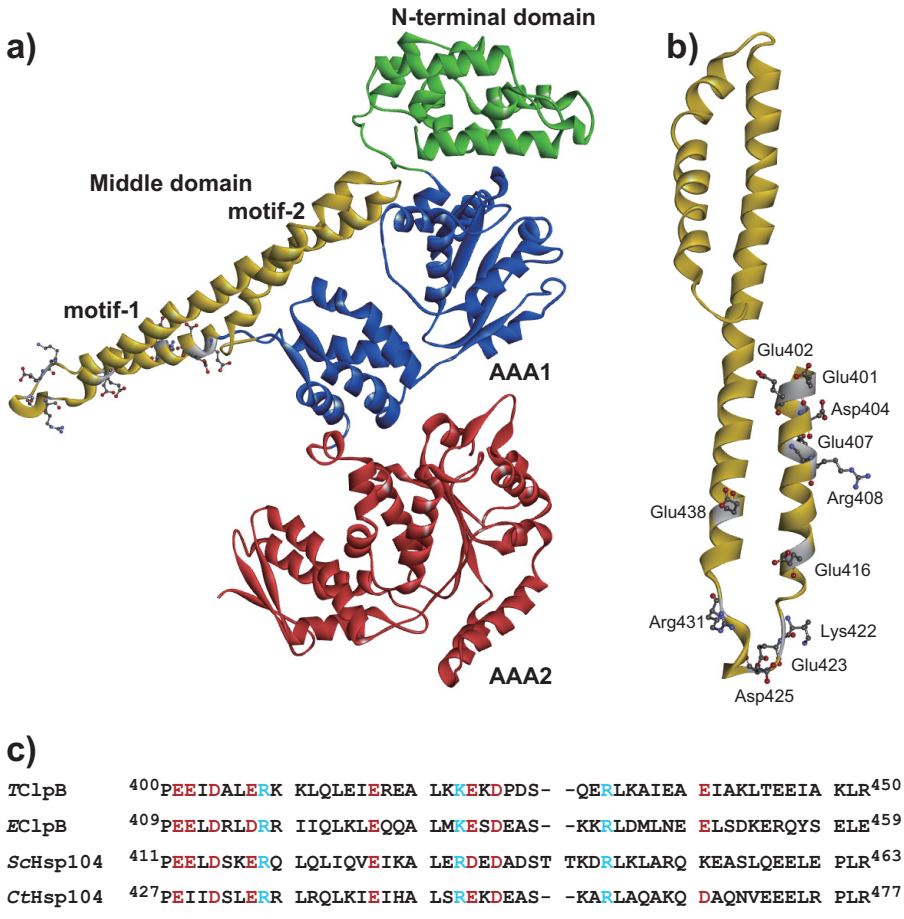

Figure 1. Positions of the mutated residues of *T*ClpB. *a*, structure of *T*ClpB (PDB code 1QVR) is shown. The N-terminal domain, AAA1, middle domain, and AAA2 are colored in *green, blue, yellow,* and *red*, respectively. *b*, structure of the *T*ClpB middle domain. The amino acid residues, Glu-401, Glu-402, Asp-404, Glu-407, Arg-408, Glu-416, Lys-422, Glu-423, Asp-425, Arg-431, and Glu-438, which were replaced by Ala, are shown as *sticks*. *c*, amino acid sequences of the middle domain motif-1 of ClpB/Hsp104 from *T. thermophilus* (*T*ClpB), *E. coli* (*E*ClpB), *S. cerevisiae* (*Sc*Hsp104), and *Chaetomium thermophilum* (*Ct*Hsp104) are aligned. The positively and negatively charged conserved residues, which were replaced by Ala, are shown in *blue* and *red*, respectively.

recruitment of ClpB/Hsp104 to aggregates and relieves repression by the MD.

Mutations at the edge of motif-1 and motif-2, E432A and Y503D of *Escherichia coli* ClpB (*E*ClpB), are known to stabilize the repressed and activated conformations, and these mutants are termed repressed and hyperactive mutants, respectively (18, 27). Single particle reconstitution of cryo-EM images of these mutants revealed that the conformations of the MD in the repressed and hyperactive mutants are horizontal and tilted to the main body, respectively (28). In the horizontal conformation, both edges of the MD interact with the MD edges of neighboring subunits in a head-to-tail manner. The interaction between the DnaK NBD and the motif-2 of ClpB MD is thought to disrupt the inter-MD interactions and induce the MD into the tilted conformation.

Although the role of MD motif-2 in binding DnaK NBD is clear, the roles of motif-1 should also be investigated to understand the mechanisms involved in controlling MD conformation, and in the regulation of ClpB activity by the MD. To clarify these issues, here we identified functionally important residues in motif-1 and their targets for interaction. We also identified the nucleotide dependence of the interactions.

Results

Effects of alanine substitutions of conserved charged residues in the ClpB MD motif-1

To identify important residues in the MD motif-1, we substituted the conserved charged residues, Glu-401, Glu-402, Asp-404, Glu-407, Arg-408, Glu-416, Lys-422, Glu-423, Asp-425, Arg-431, and Glu-438, in motif-1 with Ala and tested the effects on ClpB activities (Fig. 1, *b* and *c*).

At 55 °C, WT *T*ClpB hydrolyzed ATP at a rate of 48 min^{-1}, and the rate was stimulated by the presence of κ-casein up to 83 min^{-1} (Fig. 2*a*). All of the tested Ala mutants showed similar or at most 2-fold higher ATPase activity to that of the WT, in both the absence and presence of κ-casein (Fig. 2*a*).

The disaggregation activities were measured by using α-glucosidase from *Bacillus stearothermophilus*, which was completely aggregated by heat treatment at 73 °C for 10 min (29). The WT *T*ClpB could reactivate 54% of the aggregated α-glucosidase by incubation with *T*DnaK, *T*DnaJ, *T*GrpE (*T*KJE), and ATP at 55 °C for 90 min (Fig. 2*b*). Although the E402A, E407A, E416A, K422A, R431A, and E438A mutants showed almost the same disaggregation activity as that of WT, the reactivation yields of E401A, R408A, and D425A mutants decreased to 10,

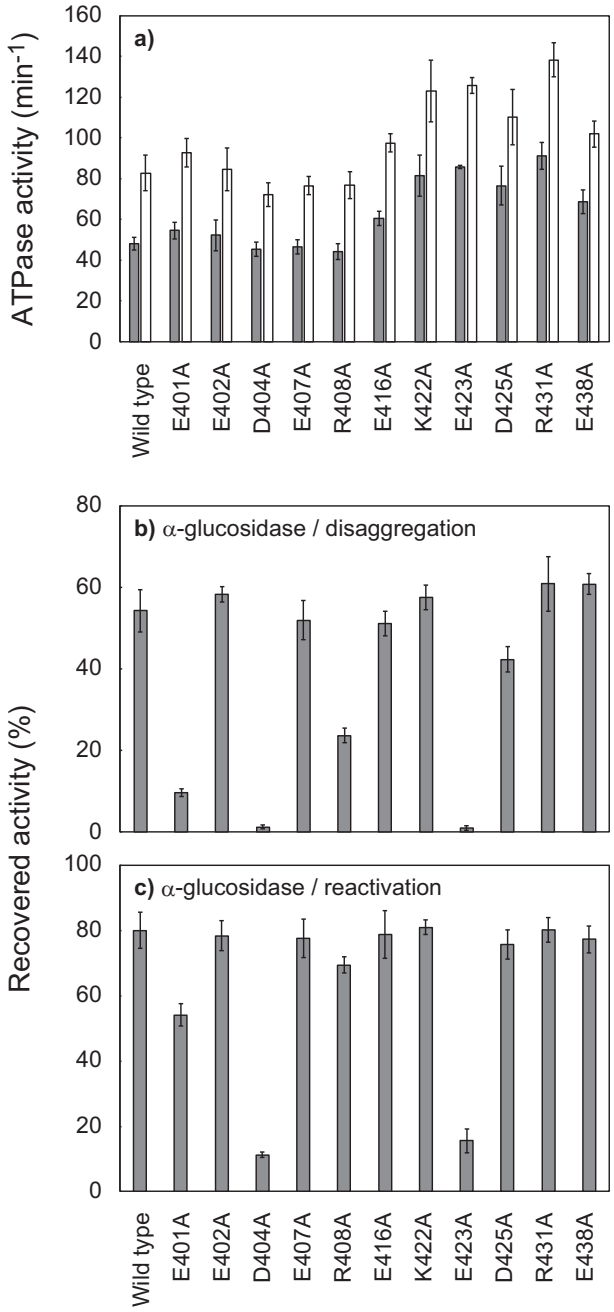

Figure 2. Effects of alanine substitutions of conserved charged residues in *T*ClpB middle domain motif-1. *a,* ATPase activities of *T*ClpB mutants, in the absence (*gray bar*) or the presence (*open bar*) of 0.1 mg/ml κ-casein, are shown as turnover number per monomer. The measurements were performed in the presence of 3 mM ATP at 55 °C using an ATP-regeneration system. *b,* disaggregation activities of *T*ClpB mutants. α-Glucosidase (final concentration, 0.2 μM monomer) was heat-aggregated by incubation at 73 °C for 10 min in the presence of 3 mM ATP. *T*DnaK (0.6 μM), *T*DnaJ (0.2 μM), *T*GrpE (0.1 μM dimer), and *T*ClpB mutants (0.05 μM hexamers) were added to the reaction mixture, and the mixture was subsequently incubated at 55 °C for 90 min. After incubation, the recovered enzymatic activities were measured and are shown as a percentage of the activities before heat aggregation. *c,* chaperone activities of *T*ClpB mutants for the reactivation of soluble, denatured proteins were measured by using α-glucosidase as a substrate. The experimental procedures were essentially the same as for *b*, except that the *T*DnaK, *T*DnaJ, and *T*GrpE were added prior to the heat treatment, and the substrate was denatured but not aggregated. *a–c, error bars* represent standard deviations of three or more independent experiments.

24, and 42%, respectively, and the D404A and E423A mutants completely lost disaggregation activity.

When the α-glucosidase was heat-treated in the presence of *T*KJE and ATP, the substrate protein lost enzyme activity (denatured); however, it remained soluble (29). The soluble, denatured protein can be reactivated by incubation at 55 °C in the presence of *T*KJE, ATP, and *T*ClpB supplemented after the 73 °C heat treatment. In this case, WT *T*ClpB could reactivate 80% of soluble, denatured α-glucosidase (Fig. 2*c*). As in the case of disaggregation, D404A and E423A mutations severely inhibited the reactivation activity. However, R408A and D425A mutants could reactivate the soluble, denatured α-glucosidase at almost the same efficiency as that of the WT, and the reactivation yield by the E401A mutant also increased, reaching 54%.

Here, we identified several important (Glu-401, Arg-408, and Asp-425) and essential (Asp-404 and Glu-423) residues for the chaperone activity of ClpB. Among these residues, the importance of Glu-423 (corresponding to Glu-432 of *E*ClpB) has been reported, and its roles have been proposed previously (18, 28). Thus, hereafter, we focused on Asp-404 and Glu-401. The former is a newly identified essential residue, and the latter is an amino acid that is more important than Arg-408 and Asp-425.

Glu-401 and Asp-404 interact with neighboring subunits

To identify the interaction targets of Glu-401 and Asp-404, we used the bidirectional photoreactive cross-linker, benzophenone-4-maleimide (BPM). The BPM-labeled *T*ClpB mutants, E401C-BPM and D404C-BPM, were UV-irradiated in the absence or presence of nucleotides and analyzed by SDS-PAGE (Fig. 3, *a* and *b*). By the UV irradiation, the intensity of the band representing noncross-linked BPM-labeled *T*ClpB decreased, and several ladder bands with higher molecular weights appeared (Fig. 3*a*). As the reaction mixture did not contain proteins other than BPM-labeled *T*ClpB, inter-subunit cross-linking would occur, and each ladder band corresponded to a multimer of BPM-labeled *T*ClpB. We quantified the intensities of bands corresponding to 1–5- and over 6-mer (Fig. 3*b*). It should be noted that the over 6-mer bands consisted of a few closely positioned bands, which would correspond to linear 6-mer, closed-ring 6-mer, or 7-mer that would appear transiently (17). When the E401C-BPM was UV-irradiated in the absence of nucleotide, the intensity of the noncross-linked 1-mer band decreased to 24%, and 31% of E401C-BPM appeared as over 6-mer band. However, intensities of the over 6-mer bands decreased to less than 4% when the UV irradiation was performed in the presence of ATP or ADP (Fig. 3, *a* and *b*). Also, in the case of D404C-BPM, similar ladder bands appeared after UV irradiation (Fig. 3, *a* and *b*). However, the nucleotide dependence was opposite that seen in the case of E401C-BPM. These results indicated that Glu-401 and Asp-404 interacted with neighboring subunits, in different ways, and these interactions were influenced by the nucleotide states.

To identify the responsible nucleotide-binding domain, similar experiments using E401C-BPM and D404C-BPM bearing mutations in the Walker-A consensus sequences of AAA1 or AAA2 were also performed (Fig. 3, *a* and *b*). Conserved Lys–Thr pairs in the Walker-A sequence (G*XX*G*X*GKT) were replaced by Ala–Ala, and the mutated AAA module could not

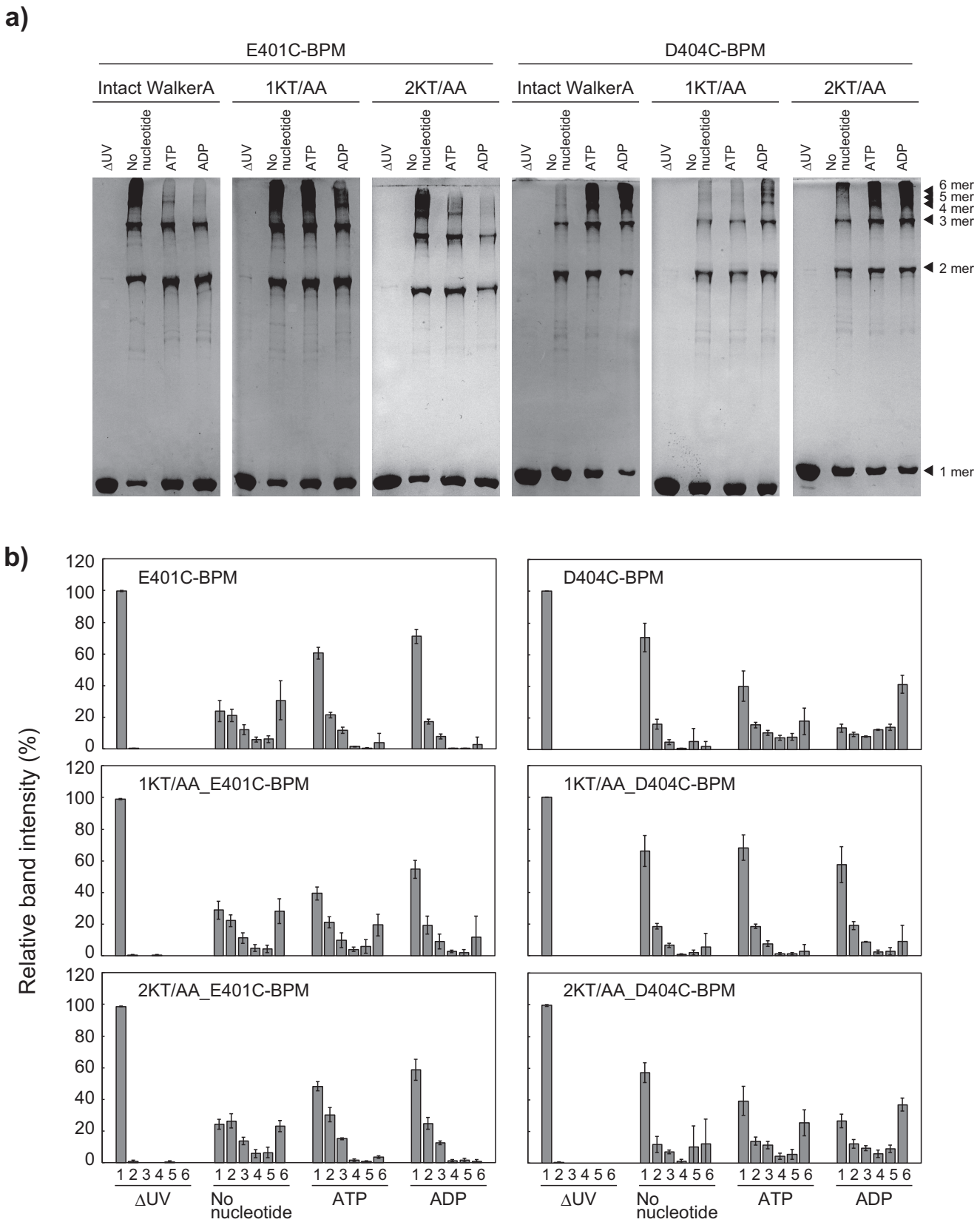

Figure 3. Essential charged residues in the middle domain motif-1 involved in nucleotide-dependent inter-subunit interactions. To form covalent bonds between the essential charged residues in motif-1 and the closely positioned C–H bond, BPM-labeled *T*ClpB mutants were UV-irradiated at 365 nm for 90 min in the absence or presence of 3 mM nucleotides. The cross-linked samples were analyzed by SDS-PAGE (5% polyacrylamide). *a*, gel images; *b*, intensities of bands corresponding to 1–5- and over 6-mers of E401C-BPM and D404C-BPM, with or without Walker-A mutations are shown. *b, error bars* represent standard deviations of three or more independent experiments.

Table 1
Cross-linked peptide pairs detected by LC-MS/MS

*T*ClpB	Nucleotide	Peptide including Cys labeled with BPM	Peptide including photo cross-linked residue	Theoretical peptide mass	No. of detected spectra
				Da	
E401C	No nucleotide	^{394}MALESAPCEIDALER^{408}	^{218}GDVPEGLK^{225}	2756.27924	12
		^{394}MALESAPCEIDALER^{408}	^{215}IVKGDVPEGLK^{225}	3096.52666	10
		^{394}MALESAPCEIDALERK^{409}	^{215}IVKGDVPEGLK^{225}	3224.62162	7
		^{392}LRMALESAPCEIDALERK^{409}	^{218}GDVPEGLK^{225}	3153.55935	5
		^{394}MALESAPCEIDALER^{408}	^{519}LEVTEEDIAEIVSRWTGIPVSK^{540}	4413.15145	8
		^{394}MALESAPCEIDALER^{408}	^{381}AIDLIDEAAARLR^{393}	3368.64995	5
	ATP	^{394}MALESAPCEIDALER^{408}	^{218}GDVPEGLK^{225}	2756.27924	7
		^{394}MALESAPCEIDALER^{408}	^{215}IVKGDVPEGLK^{225}	3096.52666	11
		^{394}MALESAPCEIDALERK^{409}	^{218}GDVPEGLK^{225}	2884.37419	2
		^{394}MALESAPCEIDALER^{408}	^{519}LEVTEEDIAEIVSR^{532}	3544.67080	2
		^{394}MALESAPCEIDALER^{408}	^{519}LEVTEEDIAEIVSRWTGIPVSK^{540}	4413.15145	12
		^{394}MALESAPCEIDALERK^{409}	^{519}LEVTEEDIAEIVSRWTGIPVSK^{540}	4541.24640	2
		^{394}MALESAPCEIDALER^{408}	^{381}AIDLIDEAAARLR^{393}	3368.64995	4
		^{394}MALESAPCEIDALER^{408}	^{392}LRMALESAPCEIDALERKK^{410}	4114.99543	2
D404C	No nucleotide	^{394}MALESAPEEICALER^{408}	^{218}GDVPEGLK^{225}	2770.29489	2
		^{394}MALESAPEEICALER^{408}	^{215}IVKGDVPEGLK^{225}	3110.54231	5
		^{394}MALESAPEEICALERKK^{410}	^{215}IVKGDVPEGLK^{225}	3366.73222	2
		^{394}MALESAPEEICALER^{408}	^{381}AIDLIDEAAARLR^{393}	3382.66560	11
		^{394}MALESAPEEICALER^{408}	^{409}KKLQLEIER^{417}	3112.56919	2
		^{394}MALESAPEEICALER^{408}	^{701}NTVIILTSNLGSPLILEGLQK^{721a}	4179.16016	4
	ATP	^{394}MALESAPEEICALER^{408}	^{215}IVKGDVPEGLK^{225}	3110.54231	6
		^{394}MALESAPEEICALERK^{409}	^{218}GDVPEGLK^{225}	2898.38984	2
		^{394}MALESAPEEICALER^{408}	^{381}AIDLIDEAAARLR^{393}	3382.66560	7
		^{394}MALESAPEEICALER^{408}	^{409}KKLQLEIER^{417}	3112.56919	2
		^{394}MALESAPEEICALER^{408}	^{835}VQVDVGPAGLVFAVPAR^{851}	3650.82315	2
		^{394}MALESAPEEICALER^{408}	^{701}NTVIILTSNLGSPLILEGLQK^{721a}	4179.16016	4

[a] MALESAPEEICALER-NTVIILTSNLGSPLILEGLQK cross-linked signals were also detected in no UV-irradiation samples.

bind nucleotides (30). In both cases of E401C-BPM and D404C-BPM, Walker-A mutations involving AAA1 were more effective than those in AAA2 in canceling the nucleotide dependence of cross-linking efficiency (Fig. 3, *a* and *b*).

Mass spectrometric analysis of cross-linked TClpB-BPM

To identify the site of cross-linkage, we performed mass spectrometric analysis of cross-linked *T*ClpBs by using LC-MS/MS (Table 1). To simplify the interpretation of MS data, ND-truncated *T*ClpB (*T*ClpB_ΔN) was used in this analysis. The *T*ClpB_ΔN_E401C-BPM, UV-irradiated in the absence of nucleotides, was cleaved by trypsin and analyzed by LC-MS/MS. We detected some peptides cross-linked by BPM. Peptides comprising the sequence from Gly-218 to Lys-225 (^{218}GDVPEGLK^{225}) of *T*ClpB were most frequently detected as the cross-linkage targets of E401C-BPM. The peptides ^{519}LEVTEEDIAEIVSRWTGIPVSK^{540} and ^{381}AIDLIDEAAARLR^{393} were also detected. When the UV irradiation was performed in the presence of ATP, a similar set of peptides was detected. In this condition, the peptides ^{519}LEVTEEDIAEIVSR^{532} (a part of ^{519}LEVTEEDIAEIVSRWTGIPVSK^{540}) and ^{392}LRMALESAPCEIDALERKK^{410} were also detected. In the cases of *T*ClpB_ΔN_D404C-BPM, UV-irradiated in the absence or presence of ATP, peptides containing the sequence ^{218}GDVPEGLK^{225}, ^{381}AIDLIDEAAARLR^{393}, ^{409}KKLQLEIER^{417}, and ^{701}NTVIILTSNLGSPLILEGLQK^{721} were detected as the cross-linkage targets. A peptide ^{835}VQVDVGPAGLVFAVPAR^{851} was detected only when the UV irradiation was performed in the presence of ATP. It should be noted that the peptide, ^{701}NTVIILTSNLGSPLILEGLQK^{721} might be mis-annotated, because the peptide was also detected in the analysis without UV irradiation.

Candidates for residues interacting with Glu-401 and Asp-404

To confirm the plausibility of the mass spectrometric analysis, we constructed hexameric structural models of *T*ClpB by homology modeling using recently solved cryo-EM structures of *E*ClpB hexamers as templates (16). Fig. 4 shows interfaces between an MD motif-1 and the AAA1 of the neighboring subunit in the *T*ClpB models. The MDs in Fig. 4, *a* and *b*, correspond to the tilted (chain D of the PDB code 5og1) and the horizontal (chain C of the PDB code 5ofo) conformation, respectively. Although inter-subunit interactions involving Glu-401 and Asp-404 were not identified in these models, the B3-helix (Asp-176–Leu-187) and the loop between the B4-helix and b3-strand (Gly-218–Lys-227) of the AAA1 large sub-domain of the neighboring subunit were found to be proximal to Glu-401 and Asp-404. This was consistent with the result that the ^{218}GDVPEGLK^{225} peptide was found as the primary cross-linking target of both E401C-BPM and D404C-BPM. On the surface of the helix and the loop, some conserved charged residues, Asp-176, Glu-177, Arg-180, Arg-181, Arg-214, Asp-219, and Glu-222, were found (Fig. 4, *a–c*). In addition, only in the tilted conformation Glu-401 was located near Arg-532 in the ^{519}LEVTEEDIAEIVSRWTGIPVSK^{540} peptide that was detected as a cross-linking target for E401C-BPM (Fig. 4, *d* and *e*). Furthermore, Arg-532 was highly conserved among various ClpB/Hsp104s (Fig. 4*f*). Considering the hexameric model, structural regions corresponding to the other detected peptides, ^{381}AIDLIDEAAARLR^{393}, ^{392}LRMALESAPCEIDALERKK^{410}, ^{409}KKLQLEIER^{417}, ^{835}VQVDVGPAGLVFAVPAR^{851}, did not seem to interact with either Glu-401 or Asp-404. Thus, we considered these conserved charged eight residues as candidates for target residues that functionally interact with Glu-401 and/or Asp-404.

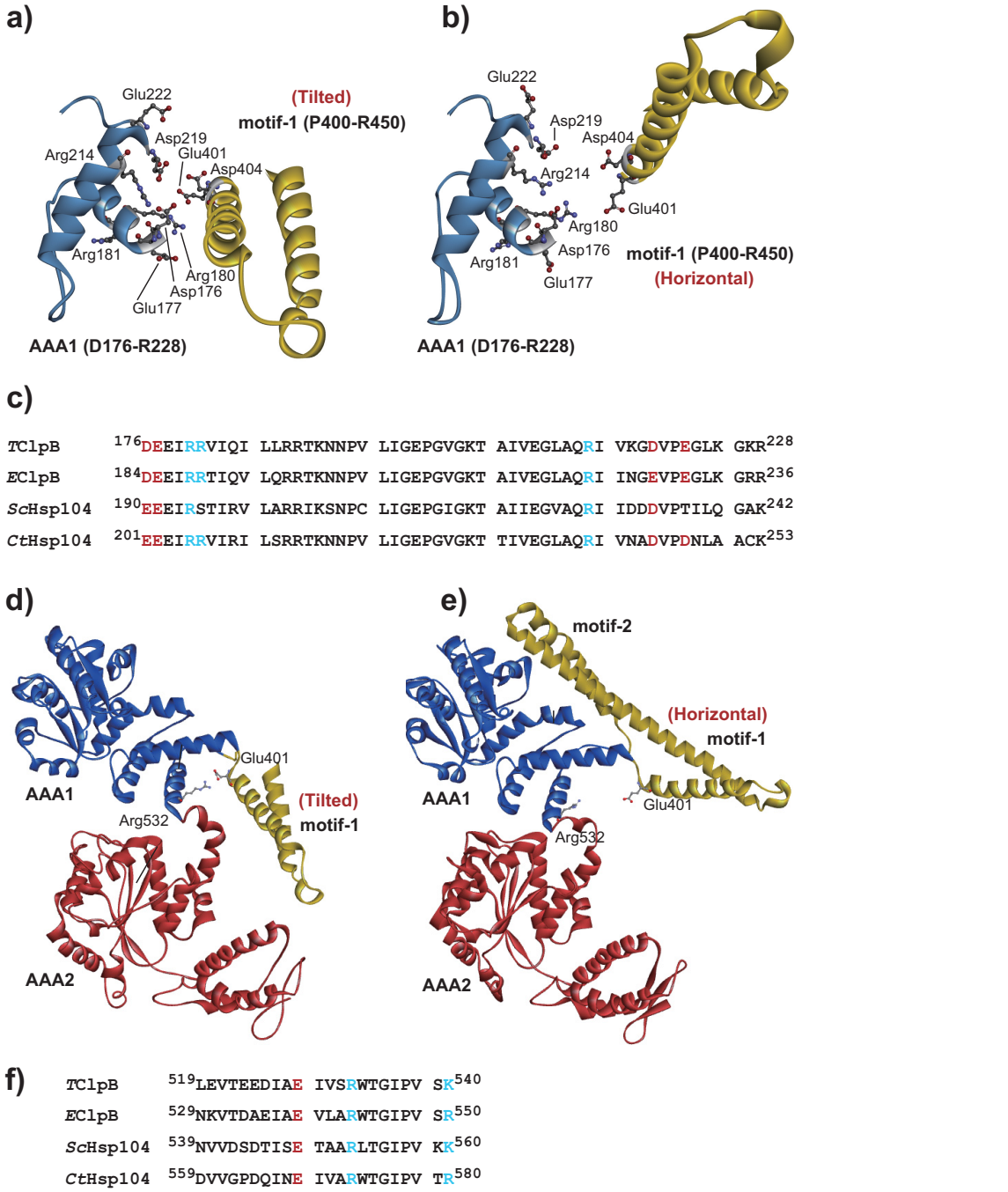

Figure 4. Structural models of *T*ClpB. The structural models of the *T*ClpB hexamer were constructed by homology modeling using cryo-EM structures of *E*ClpB with or without casein (PDB codes 5og1 and 5ofo) as templates. *a* and *b*, interfaces between AAA1 (*light blue*) and middle domain motif-1 (*yellow*) of neighboring subunits. AAA1 and motif-1 correspond to chains C and D (the middle domain is in the tilted conformation) of 5og1 (*a*), and chains B and C (the middle domain is in the horizontal conformation) of 5ofo (*b*). Amino acid residues, Glu-401, Asp-404, Asp-176, Glu-177, Arg-180, Arg-181, Arg-214, Asp-219, and Glu-222, which were replaced by Ala, are shown as *sticks*. *c*, amino acid sequences of a part of AAA1 of ClpB/Hsp104 from *T. thermophilus* (*T*ClpB), *E. coli* (*E*ClpB), *S. cerevisiae* (*Sc*Hsp104), and *C. thermophilum* (*Ct*Hsp104) were aligned. The positively and negatively charged conserved residues, which were replaced by Ala, are shown in *blue* and *red*, respectively. *d* and *e*, *T*ClpB structural model constructed based on chain D of 5og1 (*d*) and chain C of 5ofo (*e*). Amino acid residues Glu-401 and Arg-532 are shown as *sticks*. *f*, amino acid sequences of a part of AAA1 of *T*ClpB, *E*ClpB, *Sc*Hsp104, and *Ct*Hsp104 were aligned. Positively and negatively charged conserved residues are shown in *blue* and *red*, respectively.

Effects of alanine substitutions of candidate residues

We substituted these candidate residues with Ala and tested the effects on ClpB activities. D176A and E177A mutants showed 2–4 times higher ATPase activity than the WT, whereas the activities of the other mutants were similar to or slightly lower than the WT (Fig. 5*a*). D176A, E177A, and E222A mutants could reactivate aggregated and soluble, denatured α-glucosidase with efficiencies comparable with that of WT (Fig. 5, *b* and *c*). However, the other mutants hardly reactivated the aggregated α-glucosidase. The reactivation yields of soluble, denatured α-glucosidase by R180A, R181A, R214A, and D219A mutants were also relatively low, ~20–30%, whereas

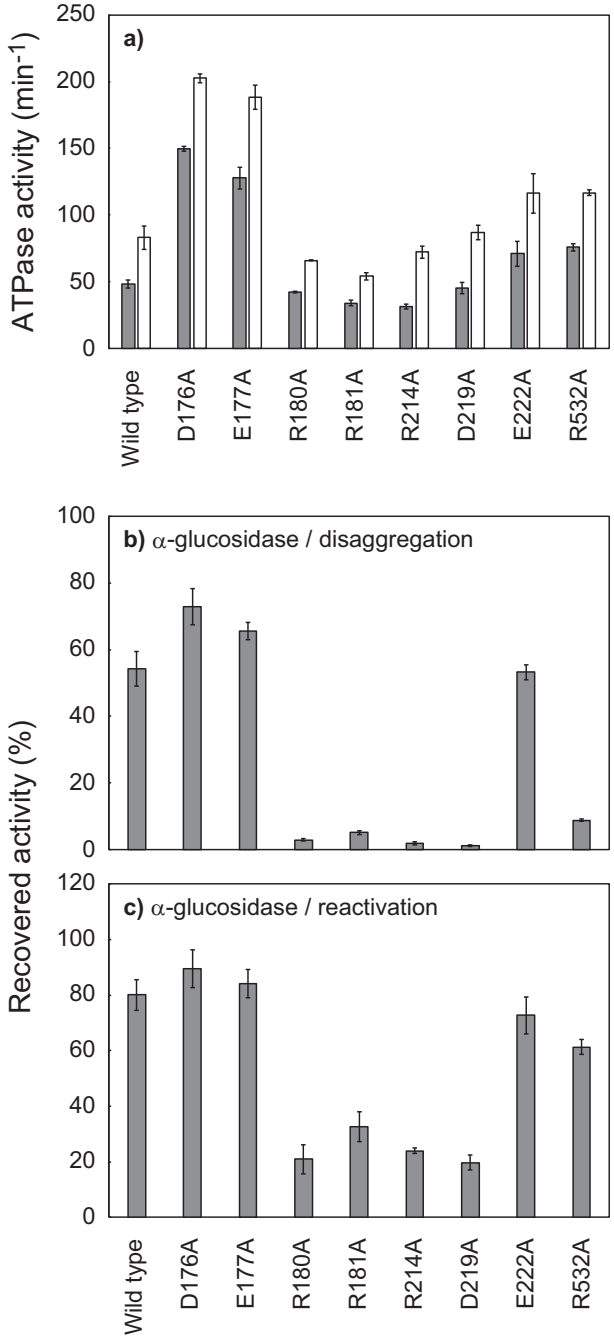

Figure 5. Effects of alanine substitutions of the charged residues in the region of AAA1 that potentially interact with Glu-401 and Asp-404. *a*, ATPase activities of *T*ClpB mutants in the absence (*gray bar*) or presence (*open bar*) of 0.1 mg/ml κ-casein are shown. *b*, disaggregation activities of *T*ClpB mutants were measured using α-glucosidase as a substrate. *c*, chaperone activities of *T*ClpB mutants for the reactivation of soluble, denatured proteins were measured by using α-glucosidase as a substrate. Experimental procedures for *a–c* were the same as for Fig. 2, *a–c*. *Error bars* represent standard deviations of three or more independent experiments.

that of R532A was considerably high at 61%, similar to the case of E401A (Fig. 5, *b* and *c*).

Effects of charge-inversion mutations

Because the effects of the R180A, R181A, R214A, D219A, and R532A mutations were similar to those of the E401A and D404A mutations, these residues might interact with Glu-401 and/or Asp-404. To test this possibility, we prepared *T*ClpB mutants in which these charged residues were substituted by amino acids having the opposite charge, and the mutations were combined. All of the single and combined charge-inverted mutants tested here showed comparable ATPase activities to that of the WT (48–150%) and 1.5–2.7-fold ATPase stimulation by κ-casein (Fig. 6, *a* and *b*). Although all the single charge-inverted mutants hardly reactivated the heat-aggregated α-glucosidase (the reactivation yields were less than 7%), the R180D_D404R and R532E_E401R double mutants could reactivate it to 31 and 25%, respectively (Fig. 6, *c* and *d*). Such recovery of disaggregation activity was not observed with any other combinations of charge-inverted mutations. Concerning the reactivation of soluble, denatured α-glucosidase, some single and combined charge-inverted mutants resulted in some extent of reactivation: R181E (34%), R181D (25%), R214E (50%), R214D (46%), R532E (41%), E401R (20%), and R214D_D404R (27%) (Fig. 6, *e* and *f*). However, compared with these mutants, R180D_D404R and R532E_E401R showed an outstanding reactivation yield of 75 and 68%, respectively, and these approached the WT level, 80%.

Discussion

Here, we tested the effects of alanine substitution of conserved charged residues in the MD motif-1 of *T*ClpB. Some Ala mutants, especially E401A, D404A, and E423A, lost their disaggregation activities, whereas their ATPase activities were maintained. Among them, Glu-423 (Glu-432 of *E*ClpB) was previously identified as a functionally-important residue and thought to be responsible for destabilizing the repressed state of ClpB (18, 28). In the recent cryo-EM structure of Hsp104 from *Saccharomyces cerevisiae* (*Sc*Hsp104), Glu-401 (Glu-412 of *Sc*Hsp104) was found to interact with Arg-180 (Arg-194 of *Sc*Hsp104), and the substitution of this residue to Lys caused a loss of chaperone activity (15). The functional importance of Asp-404 has not been reported.

The cross-linked products of E401C-BPM and D404C-BPM behaved as multimers of *T*ClpB, indicating that these residues interact with adjacent subunits. The multimeric cross-linking efficiencies of E401C-BPM and D404C-BPM were higher in the absence and presence of nucleotides, respectively. In addition, the nucleotide dependences observed in both of the mutants were weakened when nucleotide binding to AAA1 was inhibited. Moreover, LC-MS/MS analysis revealed that both E401C-BPM and D404C-BPM were cross-linked to the loop from Gly-218 to Lys-225 in AAA1. Some residues in this loop were located 5–10 Å from Glu-401 and Asp-404 in the *T*ClpB hexameric models constructed based on the cryo-EM structures of *E*ClpB (16). These results suggested that Glu-401 and Asp-404 are located near the loop when AAA1 is in the vacant or nucleotide-bound state, respectively. Nucleotide binding to AAA1 would cause sliding and/or rotational motions of the MD that could change the relative positions of these two residues at the surface of the neighboring AAA1.

In addition to the loop, the B3-helix from Asp-176 to Leu-187 was also found to be located ~5–10 Å away from Glu-401 and Asp-404. We tested the effects of alanine substitution of conserved charged residues in these loop and helix, and we

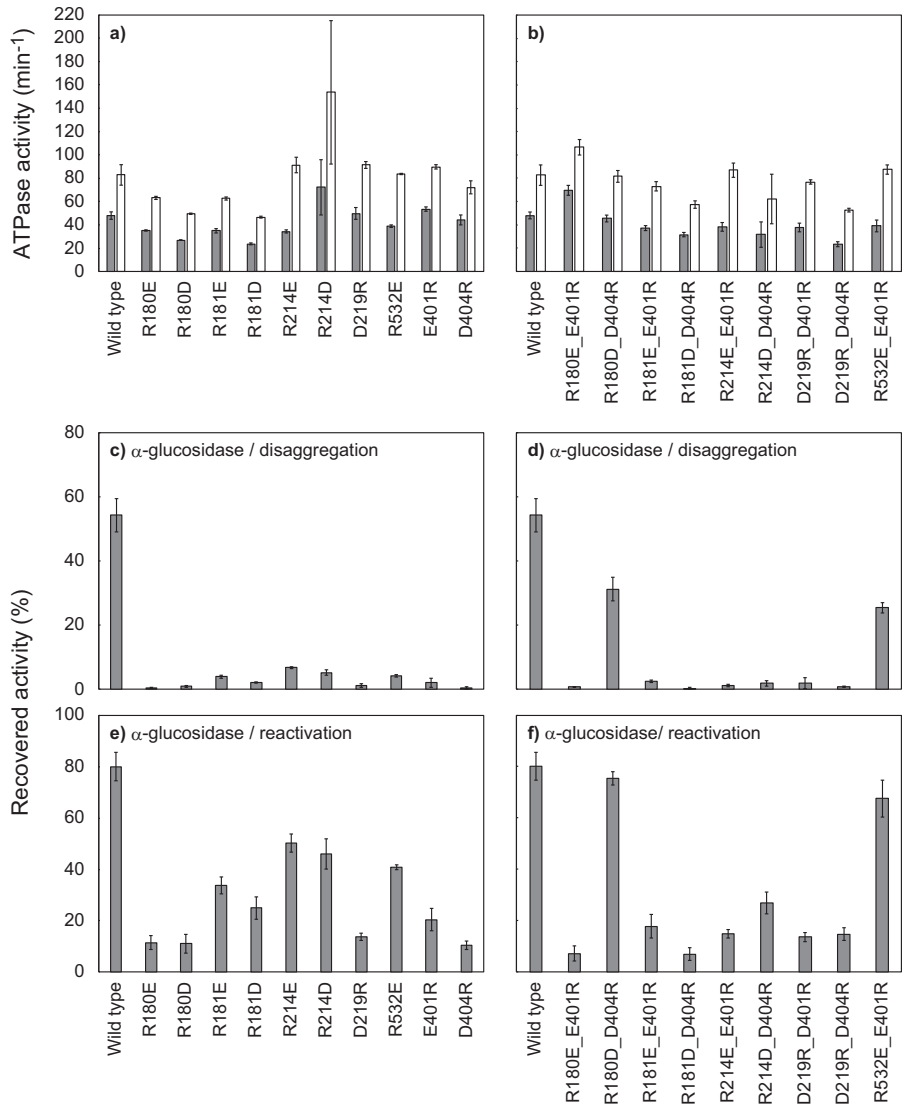

Figure 6. Effects of charge-inversion of potentially interacting pairs of amino acid residues. *a* and *b,* ATPase activities of *T*ClpB mutants having charge-inversion mutations, in the absence (*gray bar*) or presence (*open bar*) of 0.1 mg/ml κ-casein, are shown. *c* and *d*, disaggregation activities of *T*ClpB mutants were measured using α-glucosidase as a substrate. *e* and *f,* chaperone activities of *T*ClpB mutants for the reactivation of soluble, denatured proteins were measured using α-glucosidase as a substrate. *a, c,* and *e*, activities of *T*ClpB mutants having a single charge-inversion mutation. *b, d*, and *f,* activities of *T*ClpB mutants having combined charge-inversion mutations. *a–f,* experimental procedures were the same as Fig. 2, *a–c,* and *error bars* represent standard deviations of three or more independent experiments.

found that Arg-180, Arg-181, Arg-214, and Asp-219 were essential residues for the disaggregation activity of *T*ClpB. Similar to E401A and D404A, the Ala mutants of these four residues lost their disaggregation activities without losing ATPase activity. Glu-401, Asp-404, and these four residues might share a common role in disaggregation activity. The Ala substitutions of Asp-176 and Glu-177 caused the stimulation of ATPase activity and improvement of disaggregation activity, indicating that these two residues contributed to other repressive roles. Although in the cryo-EM structures of *Sc*Hsp104 and *E*ClpB, interaction between Asp-176 (Glu-190 and Asp-184 of *Sc*Hsp104 and *E*ClpB, respectively) and Arg-408 (Arg-419 and Arg-417 of *Sc*Hsp104 and *E*ClpB, respectively) was observed (14, 16), the effects of alanine substitution of these residues were opposite.

By charge exchange experiments, we tested whether functional direct interactions between the charged residues of motif-1 and neighboring AAA1 exist. The R180D_D404R double mutant showed comparable disaggregation activity compared with the WT, whereas the individual single mutants and the double mutants with other combinations lost almost all disaggregation activity. This result directly indicated that inter-subunit electrostatic interaction between Arg-180 and Asp-404 was indispensable for disaggregation activity. In the cryo-EM structure of *Sc*Hsp104, certain electrostatic interactions between charged residues in AAA1 and the MD motif-1 of neighboring subunits were shown as follows: Glu-190 and Arg-419, Arg-194 and Glu-412, Arg-353 and Glu-427, Arg-366 and Asp-434 (14, 15). However, the combination of Arg-180 and Glu-404 of *T*ClpB, corresponding to Arg-194 and Asp-415 of *Sc*Hsp104, was not found in the list. This discrepancy might be due to differences between species.

Although any additional charge-changing mutations on the loop and the helix could not restore the disaggregation activity

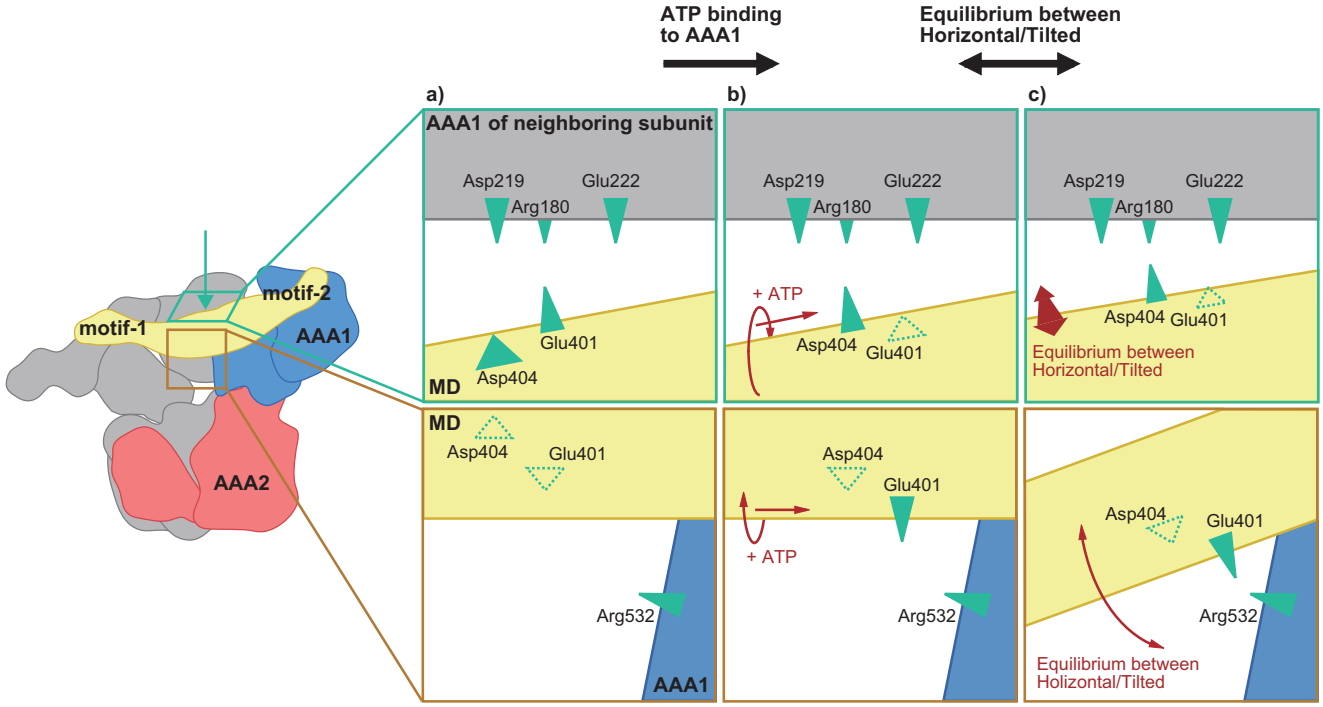

Figure 7. Schematic model of ATP-dependent changes in interactions between the middle domain motif-1 and AAA1 of neighboring subunits. *a*, Glu-401, but not Asp-404, is located near the loop, including Asp-219 and Glu-222. *b*, ATP binding to AAA1 causes sliding and/or rotational motion of the middle domain in which the Asp-404 moves close to the loop instead of Glu-401. *c*, structural change enables Glu-401 to interact with Arg-532. This interaction shifts the equilibrium of the middle domain conformation between horizontal and tilted to tilted conformation. The shift would support DnaK-induced middle domain tilting (*i.e.* ClpB activation). In the activated form, the Arg-180–Asp-404 electrostatic interaction might contribute to inter-subunit signal transduction that is essential for the chaperone activities of ClpB.

of E401R, the E401R_R532E double mutant showed substantial disaggregation activity. Arg-532 is located at the C-terminal region of AAA1 and was close to Glu-401 of the same subunit when the MD was in the tilted conformation. In addition, the ^{519}LEVTEEDIAEIVSRWTGIPVSK^{540} peptide, including Arg-532, was found as a cross-linking target for E401C-BPM but not for D404C-BPM. These results indicated that Glu-401 and Arg-532 in the same subunit constitute a functionally-important electrostatic interacting pair. It should be noted that the efficiency of inter-subunit cross-linking of E401C-BPM was relatively low in the presence of nucleotides. The cross-link between E401C-BPM and Arg-532 in the same subunit should not cause inter-subunit cross-linkage, but rather it should compete with it. Thus, the Glu-401–Arg-532 interaction would be more likely to occur in the presence of nucleotides. Indeed, the peptides containing Arg-532 were detected as cross-linking targets of E401C-BPM more frequently in the presence of ATP than in the absence of nucleotide. This interaction might support the MD in forming a tilted conformation when the AAA1 bound ATP. The other important residue on the edge of motif-1, Glu-423 (Glu-432 of *E*ClpB), was thought to destabilize the repressive horizontal conformation of the MD by preventing stable interaction between motif-1 and motif-2 of the adjacent subunits (28). The Glu-401–Arg-532 pair and Glu-423 would function complementarily.

Fig. 7 shows a possible model that was constructed based on this study. In this model, MD conformation is controlled as follows. 1) ATP binding to the AAA1 causes sliding and/or rotational motion of the MD. 2) The structural change enables Glu-401 to interact with Arg-532. This interaction shifts the equilibrium of the MD conformation between the horizontal and the tilted to the tilted. Because of this shift, when ClpB was bound to DnaK, ClpB would maintain the activated form, in which the MD is tilted, sufficiently to perform disaggregation. 3) In the activated form, the Arg-180–Asp-404 electrostatic interaction contributes to inter-subunit signal transduction that is essential for the chaperone activities of ClpB. In contrast to the mutations involving Arg-180 and Asp-404, the effects of single mutations of Glu-401 and Arg-532 on the reactivation of soluble, denatured proteins were not so severe. The equilibrium shift of MD conformations caused by these residues might contribute, in particular, to continuous generation of the mechanical power required to disentangle large insoluble aggregations.

Experimental procedures

Plasmids

The recombinant plasmid pMCB1 containing the *ClpB* gene from *Thermus thermophilus* was used as a mutagenesis template (5). Site-directed mutagenesis was performed by the overlap–extension PCR method using Ex Taq DNA polymerase (31, 32). Mutations were confirmed by DNA sequence analysis.

Proteins

Rabbit pyruvate kinase and chicken heart lactate dehydrogenase were purchased from Oriental Yeast (Tokyo, Japan). α-Glucosidase from *B. stearothermophilus* was purchased from Merck (Darmstadt, Germany). *T*ClpB and its mutants were expressed in *E. coli* BL21 (DE3) and purified as described pre-

viously (33), except that mutants with a cysteine residue were purified in the presence of 1 mM DTT. Purified *T*ClpB mutants bearing a cysteine residue were stored in a buffer containing 1 mM tris(2-carboxyethyl)phosphine hydrochloride (TCEP), at −80 °C. *T*DnaK, *T*DnaJ, and *T*GrpE were expressed in *E. coli* BL21 (DE3) carrying pMDK6 (*T*DnaK), pMDJ10 (*T*DnaJ), and pMGE3 (*T*GrpE), respectively, and purified as described previously (29, 34–36). Concentrations of substrate proteins were expressed as monomers, and those of chaperones were expressed as the monomers for *T*DnaK and *T*DnaJ, dimer for *T*GrpE, and hexamers for *T*ClpB, and its mutants.

Measurement of ATPase activity

The ATPase activities of the WT and mutant *T*ClpB were measured at 55 °C using an ATP-regenerating system containing MOPS-NaOH (pH 7.5), 150 mM KCl, 5 mM $MgCl_2$, 2 mM NADH, 50 μg/ml pyruvate kinase, 50 μg/ml lactate dehydrogenase, 2.5 mM phosphoenolpyruvate, and 3 mM ATP. The reaction was initiated by the addition of 0.05 μM WT or mutant *T*ClpB hexamers. Changes in absorbance at 340 nm were monitored using a V-650 spectrophotometer (Jasco, Tokyo, Japan).

Reactivation of aggregated α-glucosidase

α-Glucosidase (0.2 μM monomer) in a mixture containing 50 mM MOPS-NaOH (pH 7.5), 150 mM KCl, 5 mM $MgCl_2$, 3 mM ATP, and 5 mM TCEP were heat-aggregated by incubation at 73 °C for 10 min. Subsequently, chaperones (final concentration of 0.6 μM *T*DnaK, 0.2 μM *T*DnaJ, 0.1 μM *T*GrpE, and 0.05 μM WT or mutant *T*ClpB hexamers) were added to the reaction mixture. After incubation at 55 °C for 90 min, the enzymatic activities were measured as described previously (10). Disaggregation activities were expressed as percentages of the recovered enzymatic activities compared with that before heat treatment.

Reactivation of soluble, denatured proteins

To measure activities for reactivation of soluble, denatured proteins, essentially the same procedure as the disaggregation activity measurements was performed. *T*DnaK, *T*DnaJ, and *T*GrpE were added to the reaction mixtures, prior to the heat treatment. By heat treatment, the substrate proteins were denatured but not aggregated.

Labeling of TClpB mutant with BPM

*T*ClpB mutants (1–10 μM hexamer) were mixed with more than 60 molar eq of benzophenone-4-maleimide (BPM) (Merck) in 50 mM potassium phosphate buffer (pH 7.5) and incubated at 55 °C for 2 h. This buffer was replaced by the reaction buffer (50 mM MOPS-NaOH (pH 7.5), 20 mM KCl, 5 mM $MgCl_2$) by using a disposable gel-filtration column, NAP-10 (GE Healthcare, Little Chalfont, UK).

Photocross-linking of TClpB mutants

The BPM-labeled *T*ClpB mutants (0.86 μM) dissolved in buffer (50 mM MOPS-NaOH (pH 7.5), 20 mM KCl, 5 mM $MgCl_2$) were irradiated with a 365 nm UV lamp (8 watts) for 90 min at room temperature in the absence or presence of 3 mM nucleotides using an LM-20E trans-illuminator (Analytik Jena, Jena, Germany). After photocross-linking, samples were concentrated by TCA precipitation and then analyzed by SDS-PAGE on a 5.5% polyacrylamide gel and stained with Coomassie Brilliant Blue. The gel images were acquired by using ImageQuant LAS 4010 system (GE Healthcare). The intensities of bands corresponding to 1–5-and over 6-mers of *T*ClpB were quantified by using ImageQuant TL version 8.1 (GE Healthcare).

LC-MS/MS analysis

The cross-linked samples were diluted ≥5-fold with PTS solution (12 mM sodium deoxycholate, 12 mM sodium *N*-lauroyl sarcosinate, and 100 mM Tris-HCl (pH 9.0)) (37), reduced with 10 mM DTT for 30 min, and alkylated with 55 mM iodoacetamide for 30 min at room temperature. The solution was diluted 5-fold with 50 mM NH_4HCO_3, and proteins were digested by 0.25 μg of Lys-C (FUJIFILM Wako Pure Chemical, Osaka, Japan) for 3 h at room temperature. The proteins were further digested by 0.5 μg of Trypsin Gold (Promega, Fitchburg, WI) at 37 °C overnight. After digestion, the solution was acidified with 0.5% TFA (final concentration) and added to an equal volume of ethyl acetate. After vigorous mixing and centrifugation at 15,700 × *g* for 2 min, the aqueous phase was collected and dried using a centrifugal evaporator. The peptides were dissolved in 2% acetonitrile and 0.1% TFA solution and desalted with C18 Stage Tip (Nikkyo Technos, Tokyo, Japan).

Nano-LC-MS/MS analysis was performed on an Easy-nLC 1000 nanoLC system and a Q-Exactive mass spectrometer (ThermoFisher Scientific, Waltham, MA). The separation column used for the nano-LC was a 12.5 cm × 75 μm capillary column packed with 3-μm C18-silica particles (Nikkyo Technos). The separation was conducted using a 10–50% linear acetonitrile gradient at 40 min in the presence of 0.1% formic acid. The LC-MS/MS data were acquired in data-dependent acquisition mode controlled by Xcalibur 4.0 (ThermoFisher Scientific). The settings of data-dependent acquisition were as follows: the resolution was 70,000 for a full MS scan and 17,500 for MS2 scan; the AGC target was 3.0E6 for a full MS scan and 5.0E5 for MS2 scan; the maximum IT was 60 ms for both a full MS scan and MS2 scan; the scan range was 310–1,500 m/z for a full MS scan and 200–2,000 m/z for MS2 scan; and the top 10 signals were selected for MS2 scan per one full MS scan. For the detection of cross-linked peptides, the raw data were analyzed by pLink 2.0 software (38). The pLink 2.0 settings were as follows: linker mass was 295.085 Da ($C_{17}H_{11}NO_3 \cdot H_2O$), maximum missed cleavages was 3, peptide length was 5–60, mass tolerance was ± 5 ppm, separate false discovery rate was ≤1%.

Construction of structural models of TClpB hexamer

The structural models of *T*ClpB hexamers were constructed by homology modeling by using Discovery Studio 4.5 (Dassault Systemes, Velizy-Villacoublay, France). The recently solved cryo-EM structures of *E*ClpB hexamers (PDB codes 5ofo and 5og1) were used as templates (16).

Author contributions—S. S., K. W., T. N., E. U., and Y.-h. W. data curation; S. S., K. W., T. N., E. U., and Y.-h. W. formal analysis; S. S., K. W., T. N., E. U., and Y.-h. W. validation; S. S., K. W., K. H., T. N., and E. U. investigation; S. S., K. W., T. N., and Y.-h. W. visualization; S. S., K. W., T. N., and Y.-h. W. writing-original draft; T. N., H. T., and Y.-h. W. conceptualization; T. N. and Y.-h. W. methodology; T. N., H. T., and Y.-h. W. writing-review and editing; Y.-h. W. resources; Y.-h. W. supervision; Y.-h. W. funding acquisition; Y.-h. W. project administration.

References

1. Sanchez, Y., and Lindquist, S. L. (1990) HSP104 required for induced thermotolerance. *Science* **248,** 1112–1115 CrossRef Medline
2. Thomas, J. G., and Baneyx, F. (1998) Roles of the *Escherichia coli* small heat shock proteins IbpA and IbpB in thermal stress management: comparison with ClpA, ClpB, and HtpG *in vivo*. *J. Bacteriol.* **180,** 5165–5172 Medline
3. Weibezahn, J., Tessarz, P., Schlieker, C., Zahn, R., Maglica, Z., Lee, S., Zentgraf, H., Weber-Ban, E. U., Dougan, D. A., Tsai, F. T., Mogk, A., and Bukau, B. (2004) Thermotolerance requires refolding of aggregated proteins by substrate translocation through the central pore of ClpB. *Cell* **119,** 653–665 CrossRef Medline
4. Glover, J. R., and Lindquist, S. (1998) Hsp104, Hsp70, and Hsp40: a novel chaperone system that rescues previously aggregated proteins. *Cell* **94,** 73–82 CrossRef Medline
5. Motohashi, K., Watanabe, Y., Yohda, M., and Yoshida, M. (1999) Heat-inactivated proteins are rescued by the DnaK.J-GrpE set and ClpB chaperones. *Proc. Natl. Acad. Sci. U.S.A.* **96,** 7184–7189 CrossRef Medline
6. Goloubinoff, P., Mogk, A., Zvi, A. P., Tomoyasu, T., and Bukau, B. (1999) Sequential mechanism of solubilization and refolding of stable protein aggregates by a bichaperone network. *Proc. Natl. Acad. Sci. U.S.A.* **96,** 13732–13737 CrossRef Medline
7. Zolkiewski, M. (1999) ClpB cooperates with DnaK, DnaJ, and GrpE in suppressing protein aggregation. A novel multi-chaperone system from *Escherichia coli*. *J. Biol. Chem.* **274,** 28083–28086 CrossRef Medline
8. Lee, S., Sowa, M. E., Watanabe, Y. H., Sigler, P. B., Chiu, W., Yoshida, M., and Tsai, F. T. (2003) The structure of ClpB: a molecular chaperone that rescues proteins from an aggregated state. *Cell* **115,** 229–240 CrossRef Medline
9. Barnett, M. E., Nagy, M., Kedzierska, S., and Zolkiewski, M. (2005) The amino-terminal domain of ClpB supports binding to strongly aggregated proteins. *J. Biol. Chem.* **280,** 34940–34945 CrossRef Medline
10. Mizuno, S., Nakazaki, Y., Yoshida, M., and Watanabe, Y. H. (2012) Orientation of the amino-terminal domain of ClpB affects the disaggregation of the protein. *FEBS J* **279,** 1474–1484 CrossRef Medline
11. Fernández-Higuero, J. Á., Acebrón, S. P., Taneva, S. G., Del Castillo, U., Moro, F., and Muga, A. (2011) Allosteric communication between the nucleotide binding domains of caseinolytic peptidase B. *J. Biol. Chem.* **286,** 25547–25555 CrossRef Medline
12. Franzmann, T. M., Czekalla, A., and Walter, S. G. (2011) Regulatory circuits of the AAA^+ disaggregase Hsp104. *J. Biol. Chem.* **286,** 17992–18001 CrossRef Medline
13. Yamasaki, T., Oohata, Y., Nakamura, T., and Watanabe, Y. H. (2015) Analysis of the cooperative ATPase cycle of the AAA^+ chaperone ClpB from *Thermus thermophilus* by using ordered heterohexamers with an alternating subunit arrangement. *J. Biol. Chem.* **290,** 9789–9800 CrossRef Medline
14. Yokom, A. L., Gates, S. N., Jackrel, M. E., Mack, K. L., Su, M., Shorter, J., and Southworth, D. R. (2016) Spiral architecture of the Hsp104 disaggregase reveals the basis for polypeptide translocation. *Nat. Struct. Mol. Biol.* **23,** 830–837 CrossRef Medline
15. Gates, S. N., Yokom, A. L., Lin, J., Jackrel, M. E., Rizo, A. N., Kendsersky, N. M., Buell, C. E., Sweeny, E. A., Mack, K. L., Chuang, E., Torrente, M. P., Su, M., Shorter, J., and Southworth, D. R. (2017) Ratchet-like polypeptide translocation mechanism of the AAA^+ disaggregase Hsp104. *Science* **357,** 273–279 CrossRef Medline
16. Deville, C., Carroni, M., Franke, K. B., Topf, M., Bukau, B., Mogk, A., and Saibil, H. R. (2017) Structural pathway of regulated substrate transfer and threading through an Hsp100 disaggregase. *Sci. Adv.* **3,** e1701726 CrossRef Medline
17. Uchihashi, T., Watanabe, Y. H., Nakazaki, Y., Yamasaki, T., Watanabe, H., Maruno, T., Ishii, K., Uchiyama, S., Song, C., Murata, K., Iino, R., and Ando, T. (2018) Dynamic structural states of ClpB involved in its disaggregation function. *Nat. Commun.* **9,** 2147 CrossRef Medline
18. Oguchi, Y., Kummer, E., Seyffer, F., Berynskyy, M., Anstett, B., Zahn, R., Wade, R. C., Mogk, A., and Bukau, B. (2012) A tightly regulated molecular toggle controls AAA^+ disaggregase. *Nat. Struct. Mol. Biol.* **19,** 1338–1346 CrossRef Medline
19. Lipińska, N., Ziętkiewicz, S., Sobczak, A., Jurczyk, A., Potocki, W., Morawiec, E., Wawrzycka, A., Gumowski, K., Ślusarz, M., Rodziewicz-Motowidło, S., Chruściel, E., and Liberek, K. (2013) Disruption of ionic interactions between the nucleotide binding domain 1 (NBD1) and middle (M) domain in Hsp100 disaggregase unleashes toxic hyperactivity and partial independence from Hsp70. *J. Biol. Chem.* **288,** 2857–2869 CrossRef Medline
20. Acebrón, S. P., Martín, I., del Castillo, U., Moro, F., and Muga, A. (2009) DnaK-mediated association of ClpB to protein aggregates. A bichaperone network at the aggregate surface. *FEBS Lett.* **583,** 2991–2996 CrossRef Medline
21. Hayashi, S., Nakazaki, Y., Kagii, K., Imamura, H., and Watanabe, Y. H. (2017) Fusion protein analysis reveals the precise regulation between Hsp70 and Hsp100 during protein disaggregation. *Sci. Rep.* **7,** 8648 CrossRef Medline
22. Flaherty, K. M., DeLuca-Flaherty, C., and McKay, D. B. (1990) Three-dimensional structure of the ATPase fragment of a 70K heat-shock cognate protein. *Nature* **346,** 623–628 CrossRef Medline
23. Zhu, X., Zhao, X., Burkholder, W. F., Gragerov, A., Ogata, C. M., Gottesman, M. E., and Hendrickson, W. A. (1996) Structural analysis of substrate binding by the molecular chaperone DnaK. *Science* **272,** 1606–1614 CrossRef Medline
24. Kityk, R., Kopp, J., Sinning, I., and Mayer, M. P. (2012) Structure and dynamics of the ATP-bound open conformation of Hsp70 chaperones. *Mol. Cell* **48,** 863–874 CrossRef Medline
25. Zhuravleva, A., Clerico, E. M., and Gierasch, L. M. (2012) An interdomain energetic tug-of-war creates the allosterically active state in Hsp70 molecular chaperones. *Cell* **151,** 1296–1307 CrossRef Medline
26. Rosenzweig, R., Moradi, S., Zarrine-Afsar, A., Glover, J. R., and Kay, L. E. (2013) Unraveling the mechanism of protein disaggregation through a ClpB–DnaK interaction. *Science* **339,** 1080–1083 CrossRef Medline
27. Haslberger, T., Weibezahn, J., Zahn, R., Lee, S., Tsai, F. T., Bukau, B., and Mogk, A. (2007) M domains couple the ClpB threading motor with the DnaK chaperone activity. *Mol. Cell* **25,** 247–260 CrossRef Medline
28. Carroni, M., Kummer, E., Oguchi, Y., Wendler, P., Clare, D. K., Sinning, I., Kopp, J., Mogk, A., Bukau, B., and Saibil, H. R. (2014) Head-to-tail interactions of the coiled-coil domains regulate ClpB activity and cooperation with Hsp70 in protein disaggregation. *Elife* **3,** e02481 CrossRef Medline
29. Watanabe, Y. H., and Yoshida, M. (2004) Trigonal DnaK–DnaJ complex *versus* free DnaK and DnaJ: heat stress converts the former to the latter, and only the latter can do disaggregation in cooperation with ClpB. *J. Biol. Chem.* **279,** 15723–15727 CrossRef Medline
30. Watanabe, Y. H., Motohashi, K., and Yoshida, M. (2002) Roles of the two ATP binding sites of ClpB from *Thermus thermophilus*. *J. Biol. Chem.* **277,** 5804–5809 CrossRef Medline
31. Higuchi, R., Krummel, B., and Saiki, R. K. (1988) A general method of *in vitro* preparation and specific mutagenesis of DNA fragments: study of protein and DNA interactions. *Nucleic Acids Res.* **16,** 7351–7367 CrossRef Medline
32. Ho, S. N., Hunt, H. D., Horton, R. M., Pullen, J. K., and Pease, L. R. (1989) Site-directed mutagenesis by overlap extension using the polymerase chain reaction. *Gene* **77,** 51–59 CrossRef Medline
33. Watanabe, Y. H., Takano, M., and Yoshida, M. (2005) ATP binding to nucleotide binding domain (NBD)1 of the ClpB chaperone induces mo-

tion of the long coiled-coil, stabilizes the hexamer, and activates NBD2. *J. Biol. Chem.* **280,** 24562–24567 CrossRef Medline

34. Motohashi, K., Yohda, M., Endo, I., and Yoshida, M. (1996) A novel factor required for the assembly of the DnaK and DnaJ chaperones of *Thermus thermophilus*. *J. Biol. Chem.* **271,** 17343–17348 CrossRef Medline
35. Motohashi, K., Yohda, M., Odaka, M., and Yoshida, M. (1997) K^+ is an indispensable cofactor for GrpE stimulation of ATPase activity of DnaK x DnaJ complex from *Thermus thermophilus*. *FEBS Lett.* **412,** 633–636 CrossRef Medline
36. Mizutani, T., Nemoto, S., Yoshida, M., and Watanabe, Y. H. (2009) Temperature-dependent regulation of *Thermus thermophilus* DnaK/DnaJ chaperones by DafA protein. *Genes Cells* **14,** 1405–1413 CrossRef Medline
37. Masuda, T., Saito, N., Tomita, M., and Ishihama, Y. (2009) Unbiased quantitation of *Escherichia coli* membrane proteome using phase transfer surfactants. *Mol. Cell. Proteomics* **8,** 2770–2777 CrossRef Medline
38. Yang, B., Wu, Y. J., Zhu, M., Fan, S. B., Lin, J., Zhang, K., Li, S., Chi, H., Li, Y. X., Chen, H. F., Luo, S. K., Ding, Y. H., Wang, L. H., Hao, Z., Xiu, L. Y., Chen, S., Ye, K., He, S. M., and Dong, M. Q. (2012) Identification of cross-linked peptides from complex samples. *Nat. Methods* **9,** 904–906 CrossRef Medline